Coupling of zinc porphyrin dyes and copper electrolytes: a springboard for novel sustainable dye-sensitized solar cells

Alessia Colombo,[†,‡,¥] Gabriele Di Carlo,[†,‡] Claudia Dragonetti,[†,‡,¥] Mirko Magni,[†,‡] Alessio Orbelli Biroli,[¥,‡]. Maddalena Pizzotti,[†,‡,¥] Dominique Roberto,[†,‡,¥]* Francesca Tessore,[†,‡,¥] Elisabetta Benazzi,[q] Carlo Alberto Bignozzi,[q] Laura Casarin,[q] Stefano Caramori[q,]**

[†]Dipartimento di Chimica dell'Università degli Studi di Milano, [‡]UdR INSTM di Milano, via Golgi 19, 20133 Milano, Italy. [¥]Istituto di Scienze e Tecnologie Molecolari del CNR (CNR-ISTM), SmartMatLab Centre, Via Golgi 19, 20133 Milano, Italy. [q]Dipartimento Scienze Chimiche e Farmaceutiche, Università di Ferrara, Via F. di Mortara, Ferrara, Italy.

KEYWORDS

Dye-sensitized solar cells, zinc porphyrin dye, copper redox mediator, bis(phenanthroline) copper complexes, beta-substituted zinc porphyrins

ABSTRACT

Combination of β-substituted Zn^{2+} porphyrin dyes and copper-based electrolytes represents a sustainable route for economic and environmentally friendly dye-sensitized solar cells. Remarkably, a new copper electrolyte, $[Cu(2\text{-mesityl-}1,10\text{-phenanthroline})_2]^{+/2+}$, exceeds the performance reached by $Co^{2+/3+}$ and I^-/I_3^- reference electrolytes.

INTRODUCTION

With the milestone paper of Grätzel and O'Regan, Dye-Sensitized Solar Cells (DSSCs) have emerged as a realistic solution for harnessing the energy of the Sun and converting it into electricity [1]. Since then, an impressive amount of work has been carried out in order to improve the photoconversion efficiency (PCE), trying to optimize the sensitizer [2-7], and, in the last few years, the redox mediators [7-12].

Until recently, the most efficient DSSCs were based on polypyridyl ruthenium complexes as dye and the iodide/triiodide couple (I^-/I_3^-) as electrolyte [1-5]. However, the relatively high cost and environmental issues of ruthenium complexes encouraged the search for efficient noble-metal-free dyes [6,13]. By analogy with the process of solar energy collection by bacteria and plants, which have a porphyrinic core as a light-harvesting chromophore, porphyrins, with large absorption coefficients in the visible region of sunlight, have drawn attention as dyes for DSSCs [14,15]. The first investigated Zn^{2+} porphyrin dyes suffered from aggregation by π–π stacking interactions which reduced the electron injection efficiency in the TiO_2 electrode leading to a detrimental effect on the PCE [4, 16]. Besides, the interaction between the Zn^{2+} ion coordinated inside the porphyrinic core and the I_3^- species of the electrolyte promoted a fast recombination reaction with the injected electron [17-18]. The introduction of long alkoxy chains at the *ortho*-

positions of phenyl rings of *meso* push-pull Zn^{2+} porphyrins, in order to envelop the porphyrinic core, allowed to hinder these detrimental interactions thus increasing the DSSCs efficiencies [19-22]. The use of long alkoxy chains on a *meso* push-pull porphyrin with an ethyne-linked donor group led to a PCE value over 10% [19]. Efficiencies up to ca 13%, higher than those obtained with the most efficient Ru complexes, were reached by combining *meso*-disubstituted push-pull Zn^{2+} diarylporphyrins with tris(bipyridine) cobalt electrolytes which allow to significantly increase the open-circuit voltage (V_{OC}) with respect to the traditional I^-/I_3^- couple [23-24]. Also for synthetically less demanding β-substituted Zn^{2+} tetraaryl porphyrins, the presence of alkoxy chains produces a better PCE [22], but in this case their effect has never been tested with a metal-complex redox mediator.

It is important to point out that one of the key in boosting the performance of DSSCs is the enhancement of the V_{OC} which stems from the quasi-Fermi level position in the semiconductor photoanode, that can become more negative by addition of electrolyte additives such as *tert*-butylpyridine (tbp), and the level corresponding to the redox potential of the electrolyte. The most often used redox couple is I^-/I_3^- but it has many problems such as a too negative redox potential, complicated two-electron redox chemistry, corrosiveness and visible-light absorption [25]. $Co^{2+/3+}$ complexes have addressed some of these problems: they are outer-sphere one-electron redox systems with more positive and easily tunable redox potentials, providing large V_{OC}. Nevertheless, $Co^{2+/3+}$ complexes bring some issues associated with their stability, slow mass transport in the electrolyte solution and large internal reorganization energy between the high-spin d^7 and low-spin d^6 states which costs additional driving force for dye regeneration. The limitations caused by the reorganization energy are minimized by using well-designed $Cu^{+/2+}$

complexes with distorted tetragonal geometry [25]. These alternative electron shuttles are of particular interest since copper is an economic, environmental friendly metal.

Recently, in combination with both Ru^{2+} dyes and organic sensitizers, $Cu^{+/2+}$ complexes outperform not only iodine-based electrolytes [26-29] but also the $[Co(2,2'\text{-bipyridyl})_3]^{2+/3+}$ couple [30]. Fast dye regeneration and tunability of both redox potential and electron transfer rate make copper mediators prone to solve the thermodynamic and kinetic dichotomies of the device operation [31]. With the aim to synthesize mediators characterized by intermediate values of both redox potential and electron transfer kinetics to overcome this intrinsic conflict, few years ago some of us firstly proposed a new approach in designing copper-based electron mediators employing monosubstituted chelating phenanthrolines functionalized with a single bulky group [28], as a valuable alternative to redox couples based on sterically hindered 2,9-disubtituted analogues, proposed by Fukuzumi *et al.* [26] and to date largely adopted.

The above observations prompted us to couple β-substituted Zn^{2+} porphyrin dyes with Cu redox mediators as a novel route to low cost, environmental friendly DSSCs. We chose the tetraaryl Zn^{2+} porphyrin bearing the cyanoacrylic acid anchoring group at the β-pyrrolic position via an ethynylphenyl bridge (**D1**, Chart 1) instead of meso-disubstituted push-pull sensitizers due to its easier accessibility that does not prejudice its photosensitization ability [14-15, 32-34]. The presence of ortho-dodecyloxy chains, which produces the best shielding effect on the photoanode [34], enveloping the porphyrinic core was chosen in order to reduce any back electron transfer to Cu^{2+} species. The **D1** dye was combined with the new redox couple $[Cu(2\text{-mesityl-1,10-phenanthroline})_2]^{+/2+}$ (**1/2**, Chart 1), specifically designed to improve the V_{OC}. For comparison the known well performing couple $[Cu(2\text{-mesityl-4,7-dimethyl-1,10-phenanthroline})_2]^{+/2+}$ (**3/4**) [28-29] and the reference couple with 2,9-dimethyl-1,10-phenanthroline (**5/6**) [27] were also studied

along with I^-/I_3^- and $[Co(dtb\text{-}bpy)_3]^{2+/3+}$ (dtb-bpy=4,4'-di(tert-butyl)-2,2'-bipyridyl) redox couples. The **D2** dye bearing the simpler -COOH group instead of CH=C(CN)COOH was then combined with the best redox shuttle.

Chart 1. Chemical structures of the investigated three couples of copper-based redox mediators (**1-6**) and of the two tetraaryl Zn^{2+} porphyrin dyes (**D1,D2**).

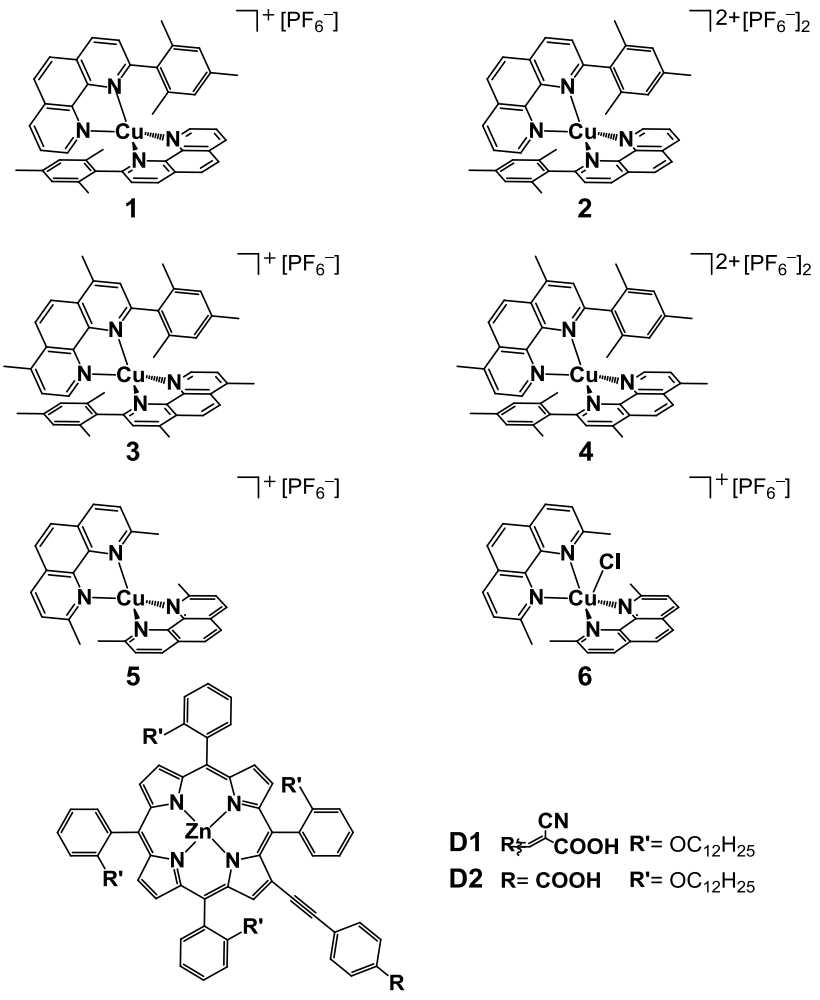

EXPERIMENTAL SECTION

General comments

All reagents and solvents were purchased by Sigma-Aldrich and used without further purification, except Et_3N (freshly distilled over KOH). 4,7-(di-methyl)-1,10-phenanthroline was purchased by Alfa Aesar. Reactions requiring anhydrous conditions were performed under argon. Glassware has been flame-dried under vacuum before use when necessary. Microwave assisted reactions were performed using a Milestone MicroSYNTH instrument.

Thin layer chromatography, TLC, was carried out with pre-coated Merck F_{254} neutral aluminium oxide 60 plates. Liquid chromatography was carried out with neutral aluminium oxide (Brockmann grade II, Alfa Aesar) or silica gel (Geduran Si 60, 63-200 μm, Merck).

^{1}H-NMR, proton decoupled ^{13}C-NMR, ^{19}F-NMR and ^{31}P-NMR spectra were recorded at T = 300 K on a Bruker Avance- DRX-400 or 300 instrument. Chemical shifts (δ) of spectra were expressed in ppm relative to Me_4Si (for ^{1}H and ^{13}C), $CFCl_3$ (for ^{19}F) and H_3PO_4 (for ^{31}P) reference compounds. Signals were abbreviated as s, singlet; d, doublet; dd, doublet of doublets; t, triplet; q, quartet; sept, septet; m, multiplet. Mass spectra, MS, were obtained with a FT-ICR Mass Spectrometer APEX II & Xmass software (Bruker Daltonics) 4.7 Magnet and Autospec Fission Spectrometer (FAB ionization) or with a Thermo-Finnigan apparatus with a Ion Trap analyzer (positive mode) and an electrospray ionization source (ESI) using a LCQ-Advantage instrument.

Elemental analysis was carried out with a Perkin-Elmer CHN 2400 instrument in the Analytical Laboratories of the Department of Chemistry at the University of Milan.

Electronic absorption spectra were recorded at room temperature in THF or acetonitrile solution, using a Shimadzu UV3600 spectrophotometer and quarz *cuvettes* with 1 cm optical

path length. Photoluminescence experiments were carried out at room temperature, in THF solution after N_2 bubbling for 120 s. Photoluminescence quantum yields were measured with a C11347 Quantaurus - QY Absolute Photoluminescence Quantum Yield Spectrometer (Hamamatsu Photonics K.K), equipped with a 150 W Xenon lamp, an integrating sphere and a multi-channel detector. Steady state emission and excitation spectra and photoluminescence lifetimes were obtained with a FLS 980 spectrofluorimeter (Edinburg Instrument Ltd.). Continuous excitation for the steady state measurements was provided by a 450 W Xenon arc lamp. Photoluminescence lifetime measurements were performed using an Edinburgh Picosecond Pulsed Diode Laser EPL-445 (Edinburg Instrument Ltd.), with central wavelength 442.2 nm and repetition rates 20 MHz, by time-correlated single-photon counting method.

Synthesis

Redox mediators

Synthesis of the new ligand 2-mesityl-1,10-phenanthroline (L1)

Ligand L1 was prepared adapting a literature procedure [28]. 2-bromo-mesitylene (2.9 mL, 19.2 mmol) was dissolved in degassed dry Et_2O (65 ml) and cooled at –78°C under an Ar atmosphere. *Tert*-butyl lithium (1.7 M in pentane) was carefully dropped (24.8 mL, 42.2 mmol). When the addition was completed the stirred solution was maintained at –78°C for 30 minutes and then it was let warmed up to r.t. over 30 minutes. The white solid product was filtered under Ar, washed with some Et_2O and dissolved, under Ar, in 20 mL of dry toluene. The white solution was dropped into a flask, filled with argon, containing a stirred solution of 1,10-phenanthroline (2.27 g, 12.6 mmol) dissolved in 260 mL of degassed dry toluene cooled to 0 °C. The solution gradually turned dark. After 20 minutes the reaction mixture was allowed to warm at r.t. and stirred overnight. The mixture was quenched with water and the organic layer was separated. The

aqueous layer was washed with dichloromethane (2 x 140 mL). The combined organic phases were dried with Na_2SO_4, filtered into a flask containing activated manganese dioxide (35.0 g, 403 mmol) and stirred at r.t. overnight. The mixture was filtrated on a celite plug and the solvent was evaporated at reduced pressure. The whitish crude product was purified by liquid chromatography on neutral Al_2O_3 through a gradient elution (from CH_2Cl_2/toluene 7:3 to pure CH_2Cl_2). Pure L1 was obtained as a white/yellow solid (1.5 g, 40 % yield).

^{1}H-NMR (400 MHz, $CDCl_3$) δ(ppm): 9.28 (dd, J_2 = 4.4 Hz, J_3 = 1.6 Hz, 1H), 8.39 (dd, J_2 = 8.0 Hz, J_3 = 1.6 Hz, 1H), 8.33 (d, J_2 = 8.2 Hz, 1H), 7.95 (d, J_2 = 8.8 Hz, 1H), 7.88 (d, J_2 = 8.8 Hz, 1H), 7.71 (dd, J_2 = 8.0 Hz, J_3 = 4.4 Hz, 1H), 7.57 (d, J_2 = 8.2 Hz, 1H), 6.89 (s, 2H), 2.36 (s, 3H), 1.97 (s, 6H).

*Synthesis of the new Cu(I) complex **1***

The precursor CuI (70 mg, 0.366 mmol) was dissolved under argon in 8 mL of acetonitrile and added dropwise to a stirred solution of the ligand L1 (224 mg, 0.751 mmol) dissolved in 20 mL of acetonitrile, under inert atmosphere. The solution instantaneously turned red and it was stirred at room temperature for *ca.* 30 minutes. The solvent was eliminated under reduced pressure; the light red solid was dissolved in the minimum amount of a 1:2 mixture H_2O/EtOH (*ca.* 60 mL) under vigorous stirring. 2 mL of an aqueous solution of $NaPF_6$ (141 mg, 2.3 eq.) was added and immediately a red precipitate was formed as a consequence of anion exchange. After 2 hours the solid was filtered off, washed with H_2O and Et_2O and, finally, dried under vacuum for some hours, until a red powder of compound **1** was obtained (252 mg, 85 % yield). Attempt to obtain crystals suitable for X-ray structural characterization failed.

^{1}H-NMR (300 MHz, CD_3CN) δ(ppm): 9.03 (dd, J_2 = 4.8 Hz, J_3 = 1.3 Hz, 2H), 8.62-8.57 (m, 4H), 8.11 (d, J_2 = 9 Hz, 2H), 8.06 (d, J_2 = 9 Hz, 2H), 7.88 (dd, J_2 = 8.2 Hz, J_3 = 4.8 Hz, 2H), 7.59

(d, J_2 = 8.2 Hz, 2H), 6.12 (s, 2H), 5.79 (s, 2H), 1.94 (s, 6H, partially hidden by solvent signal), 1.69 (s, 6H), 1.00 (s, 6H); ^{13}C-NMR APT (75 MHz, CD_3CN) δ(ppm): 158.7 (C), 149.4 (CH), 144.1 (C), 143.9 (C), 137.8 (CH), 137.5 (C), 136.5 (CH), 135.9 (C), 135.1 (C), 133.4 (C), 129.6 (C), 128.4 (CH), 127.9 (C), 126.9 (3CH), 126.7 (CH), 126.0 (CH), 20.3 (CH_3), 19.7 (CH_3), 19.1 (CH_3); ^{19}F-NMR (282 MHz, CD_3CN) δ(ppm): –73.2 (d, J_{F-P}= 704 Hz, 6F); ^{31}P-NMR (121 MHz, CD_3CN) δ(ppm): –144.0 (sept, J_{P-F}= 704 Hz, 1P). The HSQC (^{1}H-^{13}C) spectrum of complex **1** is reported in Figure S1 of the Supporting Information.

Elemental analysis calcd (%) for $C_{42}H_{36}CuF_6N_4P$: C, 62.64; H, 4.51; N, 6.96. Found C, 62.69; H, 4.52; N, 6.94.

MS (ESI^+) *m*/*z*: 659.61 (659.22 calculated).

*Synthesis of the new Cu(II) complex **2** and the known complex 4*

The two complexes were prepared following a reported procedure [29], here described for **2**.

$CuSO_4 \cdot 5H_2O$ (12.5 mg, 0.050 mmol) was dissolved in 1.5 mL of water and added to a stirred solution of 2-mesityl-1,10-phenanthroline (30 mg, 0.100 mmol) in 6 mL of acetonitrile. The solution immediately turned light green and it was stirred at room temperature for 1 hour. The solution was concentrated under reduced pressure to eliminate acetonitrile and about 1.5 mL of EtOH was added to completely dissolve the green solid. A green precipitate was immediately formed after the dropwise addition of $NaPF_6$ (35 mg, 0.210 mmol) in 1 mL of H_2O and the suspension was allowed to stir for 2 hours. The product was collected by filtration, washed with H_2O and Et_2O and, finally, dried under vacuum for some hours. Complex **2** resulted as a light green powder (29 mg, 72% yield).

Elemental analysis calcd (%) for $C_{42}H_{36}CuF_{12}N_4P_2$: C, 53.09; H, 3.82; N, 5.92. Found C, 53.13; H, 3.83; N, 5.94.

MS (ESI^+) *m*/*z*: 659.47 (659.22 calculated).

Synthesis of the known copper complexes ***3, 5, 6****, [Co(dtb-bpy)$_3$][OTf]$_2$ and [Co(dtb-bpy)$_3$][PF$_6$]$_3$*

3 and **5** were synthesized according to the same procedure described for **1**, using 2-mesityl-4,7-dimethyl-1-10-phenanthroline, prepared as previously reported [28], or commercially available 2,9-dimethyl-1,10-phenanthroline as ligand, respectively. The red products were isolated in 86% and 87% yields, respectively. ^{1}H-NMR spectra were in perfect agreement with literature [28].

Complex **6** [27,29], [Co(dtb-bpy)$_3$][OTf]$_2$ [35] and [Co(dtb-bpy)$_3$][PF$_6$]$_3$ [35] were synthesized as previously reported.

Dyes

D1 was prepared as previously reported [34] whereas **D2** ([2-(4'-Carboxyphenylethynyl)-5,10,15,20-tetrakis(2-dodecyloxyphenyl)porphyrinate]Zn^{II}) was prepared as follows. In an anhydrous Schlenk tube, under nitrogen atmosphere 107.6 mg of 4-ethynylbenzoic acid (736.3 μmol, 5 equiv.), 17.0 mg of Pd(PPh$_3$)$_4$ (14.7 μmol, 0.1 equiv.) and 220.1 mg of [2-bromo-5,10,15,20-tetrakis(2-dodecyloxyphenyl)porphyrinate]Zn^{II} (147.3 μmol, 1 equiv.), prepared as previously reported [34], were dissolved in 5 ml of anhydrous DMF over molecular sieves and 15 ml of Et$_3$N. The reaction mixture was de-aerated with three freeze-pump-thaw cycles at about -96°C, using a bath of liquid nitrogen and acetone. The solution was allowed to warm to room temperature and transferred, under nitrogen flow, into a microwave quartz vessel. 4.2 mg of CuI (22.1 μmol, 0.15 equiv.) was added and after an additional bubbling of nitrogen for 15 min, the reaction was heated at 120 °C in a microwave cavity for 1 h. The solvents were removed in vacuo and the crude product was dissolved in CH_2Cl_2 again and washed with H_2O acidified

with H_3PO_4, the organic phase was dried over anhydrous Na_2SO_4, filtered and concentrated to dryness. The crude product was purified by column chromatography on silica (CH_2Cl_2/MeOH 97.5:2.5 gradient to 95:5), obtaining 116.2 mg of product (yield 50.6 %).

^{1}H-NMR (400.1 MHz, $CDCl_3$) δ, ppm: 9.20 (1H, m), 8.78 (6H, m), 8.01 (4H, m), 7.74 (3H, m), 7.54 (5H, m), 7.34 (7H, m), 7.23 (1H, m), 3.89 (8H, m), 1.40-0.5 (92H, m).

Elemental analysis calcd (%) for $C_{101}H_{128}N_4O_6Zn$: C 77.79, H 8.27, N 3.59; found C 77.56, H 8.29, N 3.58.

MS-ESI(+) m/z: ca1cd for $C_{101}H_{128}N_4O_6Zn$ 1556, found 1557 $[M+H]^+$.

Characterization

Electrochemical measurements

Cyclic voltammetry, CV, and electrochemical impedance spectroscopy, EIS, for the electrochemical characterization of Zn-porphyrin dyes and of copper and cobalt-based complexes were performed in a three-electrode customized minicell filled with 2-4 mL of a solution of a suitable solvent with tetrabutylammonium hexafluorophosphate, $TBAPF_6$ (≥98.0 %, Sigma-Aldrich), acting as supporting electrolyte. The working solution was well deareated by bubbling nitrogen before each measure starts and blowing it over the surface of the solution during the scans.

Teflon-embedded glassy carbon electrodes, GC (geometric surface area 0.071 cm^2, purchased by Metrohm and Amel), were used as working electrode in combination with a platinum wire as counter electrode and a saturated calomel electrode, SCE, as reference one. To avoid water and chloride leakage into the working solution, SCE was inserted into a double bridge ending with a porous frit and filled with the same blank electrolytic solution (*i.e.* solvent and supporting electrolyte). The recorded potentials were subsequently referred to the intersolvental reference

redox couple Fc^+|Fc (ferricenium|ferrocene) added as external standard (*ca.* $1 \cdot 10^{-3}$ M) at the end of each daily measure.

The measures were performed with a potentiostat/galvanostat PGSTAT302N (Metrohm Autolab, The Netherlands) controlled by a PC through GPES and NOVA 1.10 software, equipped with a frequency response analyzer module (FRA2) for EIS measurements. Staircase CV were performed at different sweep potentials (0.02-2 V s^{-1}) with a potential step of 0.001-0.002 V. An instrumental compensation of the resistance (*i.e.* positive feedback) was carefully performed in order to minimize the ohmic drop between the working and reference electrode.

The determination of redox potential of electrolytes were carried out with the same setup, recording CV of a Fc solution at 0.2 V s^{-1} (see below for more details).

EIS spectra of Cu complexes were recorded superimposing to a continuous potential bias set at the half-wave potential, $E_{1/2}$, a sinusoidal alternating potential signal of 0.01 V amplitude and frequency ranging from $1 \cdot 10^4$ to $1 \cdot 10^{-1}$ Hz. Sixty logarithmically distributed single sine frequencies were employed for recording each spectrum. NOVA 1.10 software was used to validate EIS data (through Kronig-Kramers analysis) and to fit them with a Randles-type equivalent circuit to estimate the charge transfer resistance, R_{ct}, at the electrolyte/electrode interface. R_{ct} was related to heterogeneous electron transfer rate constant, k_{heter}, according to the following equation

$$k_{heter} = \frac{i_0}{FC_{Rd}} = \frac{RT}{F^2 R_{ct} C_{Rd}}$$

where i_0 is the exchange current density, F the Faraday constant, C_{Rd} the concentration of the reduced complex (in mol cm^{-3}), R is the gas constant, T the absolute temperature. In our experimental conditions temperature is about $T = 295 \pm 2$ K.

Photoelectrochemical measurements

Photoanodes were prepared by a simple procedure. FTO glass plates were washed in 2-propanol for 10 min using an ultrasonic bath, then were heated at 450°C for 20 minutes. A compact TiO_2 blocking underlayer was prepared by spin-coating a 0.3 M titanium tetraisopropoxide solution in 1-butanol (1000 rpm for 10 s, 2000 rpm for 20 s). Then the substrates were heated at 500 °C for 15 min. The photoelectrodes were prepared by doctor blading, using a transparent anatase paste composed of 20 nm nanoparticles (Dyesol 18NRT). The coated films were heated to 500 °C for 10 min with programmed temperature ramping. After sintering, the electrodes were treated with 0.4 M $TiCl_4$ overnight and heated again at 450° for 30 minutes. Once cooled, the electrodes were immersed in a 0.2 mM solution of the dye (D1 and D2) in ethanol/tetrahydrofuran 9:1, containing chenodeoxycholic acid 1 mM.

The PEDOT counter electrodes were prepared by electrodeposition through cyclic voltammetry technique, scanning 2 times from 0 to 1.7 V *vs* SCE at 20 mV s^{-1} in a 0.01 M EDOT acetonitrile solution with 0.1 M $LiClO_4$ as supporting electrolyte. The PEDOT-modified FTO were then thoroughly washed with fresh acetonitrile and dried in air.

DSSCs were finally assembled by sealing the sensitized photoanode and a poly(3,4-ethylendioxythiophene)-modified FTO counter electrode through a mask of 25 μm ionomer resin (Surlyn®, DuPontTM), properly pressed and warmed. Electrolyte was injected by a syringe through one of two holes pre-drilled on the counter electrode, that were finally sealed.

Electrolytes were all formulated using acetonitrile as solvent, 0.1 M lithium triflate (LiOTf) and 0.25 M *tert*-butyl pyridine (tbp) as additives. A 10:1 molar ratio was chosen for reduced and oxidized species of each redox couple, respectively. Thus, copper electrolytes (**1/2**-El, **3/4**-El and **5/6**-El; where El means electrolyte) were prepared dissolving the redox couple (0.17M

Cu^{+}/0.017M Cu^{2+}) in CH_3CN with 0.1 M lithium trifluoromethanesulfonate as supporting salt and 0.25 M 4-*tert*-butylpyridine as additive to improve the V_{OC} of the devices. Control electrolytes I^-/I_3^--El and Cobalt-El were prepared with a comparable amount of electroactive species: 0.17 M I^- (0.1 M LiI + 0.07 1-propyl-3-methylimidazolium iodide)/0.017 M I_2 and 0.17 M $[Co(dtb\text{-}bpy)_3]^{2+}$/0.017 M $[Co(dtb\text{-}bpy)_3]^{3+}$, respectively.

Current−voltage measurements (scan rate of 10 mV s^{-1}), chopped chronoamperometric measurements (at short circuit, *i.e.* E_{bias}= 0), open circuit voltage decay OCVD (at 50 mV sampling resolution) and electrochemical impedance spectroscopy EIS (fifty single sine frequencies logarithmically distributed between 100kHz to 10 mHz, 10 mV amplitude) were performed with a PGSTAT302N potentiostat/galvanostat equipped with a frequency response analyzer module and controlled by NOVA or GPES software (Metrohm Autolab). Cell performances were evaluated under 100 mW cm^{-2} AM 1.5 illumination (ABET sun simulator). EIS spectra were then properly fitted using ZView software (Scribner Associates, Inc.).

IPCE spectra were determined in sandwich DSSCs under short circuit conditions by using a previously described apparatus [36] by sampling the visible spectrum (400-800 nm) at 20 nm intervals with a spectral bandwidth of 10 nm. Incident irradiance was measured with a in-house calibrated silicon photodiode.

Transient absorption spectroscopy measurements

Transient absorption spectroscopy, TAS, was performed with a previously described apparatus [37] by using the 532 nm harmonic of a nanosecond Nd:YAG laser (Continuum Surelite II). A typical pulse energy of 2 mJ cm^{-2} was used. A 532 nm notch filter prevented laser light from reaching the photomultiplier, whereas a 420 nm cut-off filter, placed in front of the white light

probe beam prevented direct TiO_2 excitation. From 10 to 30 laser shots, at a frequency of 0.2 Hz were averaged to reach a good S/N ratio.

The photoelectrodes were prepared by doctor-blading TiO_2 18NRT paste on FTO substrates. After a programmed ramp heating up to 500°C the $TiClO_4$ treatment was applied, by immersing the electrodes in a 0.4 M acqueous solution overnight, after which they were heated at 450°C for 30 minutes. Then the electrodes were put in a ethanol/tetrahydrofuran 9:1 D1 solution overnight for the sensitization.

TAS measurements on transparent thin films in the presence of the electron donor species in acetonitrile were performed by drawing the electrolyte by capillarity inside the chamber (ca. 6−8 μm), constituted by a glass slide pressed against the TiO_2 photoanode. Thus, the negligible optical path allowed to avoid interferences originated by the mediators absorbance.

Regeneration efficiency was calculated by applying the formula

$$\eta = \frac{k'_{reg}}{k'_{reg} + k'_{rec}}$$

where the first order recombination, k'_{rec}, and pseudo-first order regeneration, k'_{reg}, rate constants were obtained by fitting the experimental decay curves with a biexponential function

$$y = A_1 \exp(-x/t_1) + A_2 \exp(-x/t_2) + y_0$$

following the equation

$$k' = \left(\frac{A_1 t_1^2 + A_2 t_2^2)}{A_1 t_1 + A_2 t_2} \right)^{-1}$$

The following solutions were tested :

0.1M LiOTf in acetonitrile (blank)

0.146M 1-propyl-3-methylimidazolium iodide, 0.024M LiI, in acetonitrile (I^-)

0.17M $[Co(dtb\text{-}bpy)_3](OTf)_2$, 0.1 M LiOTf , in acetonitrile (Co)

0.17 M **1**, 0.1 M LiOTf , in acetonitrile (**1**)

0.17 M **3**, 0.1 M LiOTf , in acetonitrile (**3**)

0.17 M **5**, 0.1 M LiOTf , in acetonitrile (**5**)

where LiOTf or LiI salts were employed as sources of Li^+ ions.

Determination of the redox potential of electrolytes

The redox potential of the electrolytes, E_{redox}, was experimentally determined through three-electrode voltammetric measurements recording a cyclic voltammogram of a solution containing *ca.* 0.001 M Fc dissolved in acetonitrile with 0.1 M tetrabutylammonium hexafluorophosphate as supporting salt. A glassy carbon electrode was employed as working electrode, a platinum wire as counterelectrode and an electrode filled with the tested DSSC electrolyte as reference electrode. The redox reference electrode was prepared by filling a small glass tube ending with a porous frit (assuring the electric contact) with about 100 µl of the solution then employed in DSSC, and tipping in it a well polished platinum wire. After each measurement the wire was rinsed with fresh acetonitrile and deionised water, then tipped for some minutes in concentrated HNO_3, abundantly rinsed with water, then sonicated in water and finely dried.

In this way the half-wave potential of $Fc^+|Fc$, $E_{1/2,Fc+/Fc}$, was detected respect to the E_{redox} of the tested electrolyte. So the redox potential of the electrolyte (referred to $E_{1/2}$ of $Fc^+|Fc$) corresponds to $E_{redox} = -E_{1/2,Fc+/Fc}$. It is correlated to the energy of its Fermi level, $U_{F,redox}$, by the equation

$$U_{F,redox} = -e(E_{redox} + 4.8)$$

where e=1 C and 4.8 stands for the recommended redox potential (in volt) of the ferrocenium/ferrocene, $Fc^+|Fc$, couple *versus* vacuum [38].

The knowledge of E_{redox} is also useful as a "reference potential", to properly compare results obtained from two-electrode cells when a bias potential is applied. In a DSSC the applied potential is $E_{bias}=E_{photoanode}-E_{cathode}$, where $E_{photoanode}$ is the potential of the quasi-Fermi level of electron in TiO_2, and $E_{cathode}$ is actually E_{redox}. By referring $E_{photoanode}=E_{Fn}$ to the proper E_{redox} it is possible to compared at a fixed potential (and hence energy) the DSSC features, evidencing intrinsic differences in behaviour due to different electrolytes. In doing so experimental E_{bias} is previously corrected for ohmic drop between anode and cathode ($E_{drop}=IR_{drop}$) according to $E_{corr}=E_{bias}+E_{drop}$, being E_{bias} negative.

Determination of the conduction band edge energy

Conduction band edge energy, U_{cb}, at open circuit was estimated according to the following equation [39]:

$$n_{cb} = N_{cb} \exp\left(\frac{U_{Fn} - U_{cb}}{k_b T}\right)$$

with k_b the Boltzmann constant, T the absolute temperature, N_{cb} the density of states calculated as $N_{CB} = 2\left(\frac{m_e^* k_b T}{2\pi\eta^2}\right)^{3/2}$ (where $m_e^*=2.3m_e$ was selected as the effective mass of an electron) and n_{cb} the concentration of conduction band electrons calculated according to $n_{cb} = k_b T C_\mu / e^2$ (with e the elementary charge) from the chemical capacitance of TiO_2 film (C_μ) at V_{oc} under full sunlight illumination, obtained by EIS fitting and considering 10 μm as film thickness and a 50% porosity.

Due to uncertainty on m_e^* (in literature it varies from 1 to 10-fold m_e) the reported values have a systematic error of about ±40 meV.

RESULTS AND DISCUSSION

The new compound 2-mesityl-1,10-phenanthroline was synthesized as reported for related ligands [28] whereas copper complexes were obtained by reacting the adequate phenanthroline with CuI (**1, 3, 5**), $CuSO_4.5H_2O$ (**2, 4**) or $CuCl_2.2H_2O$ (**6**), as described in the Experimental Section. The reference couple $[Co(dtb\text{-}bpy)_3]^{2+/3+}$ was prepared according to literature [35]. The new Zn^{2+} porphyrin dye **D2** was prepared adapting the procedure developed for **D1** [34] (see Experimental Section).

The absorption spectrum of the new complex **1** in acetonitrile shows a broad band centred at 451 nm (logε = 3.62) due to a metal-to-ligand charge transfer transition, in agreement with related **3** and **5** exhibiting λ_{max} at 445 nm (logε = 3.64) and 455 nm (logε = 3.90), respectively [28-29]. Its oxidized form **2** exhibits less intense transitions centred around 696 nm (logε =2.18), like **4** and **6** with λ_{max} at 697 nm (logε = 2.0) and 741 nm (logε = 2.3), respectively [29] (Figure S2). The absorption and emission properties of the new porphyrin dye **D2** are similar to those previously reported for **D1** (Table 1; Figures S3,S4,S5). The 100-fold higher absorption of dyes respect to redox mediators minimizes the light harvesting competition.

Table 1. Absorption and emission data of **D1** and **D2**.

Dye	λ_B/nm(log ε)	λ_Q/nm (log ε)	λ_{ex}/nm	λ_{em}/nm	Φ/%[a]	τ/ns[a]
D1[b]	438 (5.17)	566 (4.58) 604 (4.35)	439	616 671	3.8	2.38
D2	438 (5.48)	566 (4.32) 604 (4.00)	438	617 672	4.0	2.16

[a] Values recorded at 10^{-6} M. [b] Reference 34.

Cyclic voltammetry, CV, and electrochemical impedance spectroscopy, EIS, revealed a quite different electrochemical behaviour of the redox mediator metal complexes. In acetonitrile with 0.1 M tetrabutylammonium hexafluorophosphate as supporting electrolyte, they exhibited a metal-centred process with half-wave potential, $E_{1/2}$, of –0.21, –0.02, 0.06, and 0.30 V *vs* $Fc^+|Fc$ for $[Co(dtb\text{-}bpy)_3]^{2+}$, **3**, **1**, and **5**, respectively (Supporting Information; Table S1 and Figures S6,S7). As expected for the absence of electron releasing methyl groups in the 4,7 positions of the phenanthrolines [31], the new complex **1** exhibits a 0.08 V positively shifted $E_{1/2}$ respect to related **3**. Interestingly, all investigated Cu^+ complexes present higher oxidation potentials than $[Co(dtb\text{-}bpy)_3]^{2+}$, an intriguing features for maximization of the open circuit potential, V_{oc}, of photoelectrochemical devices. They also present a faster heterogeneous electron transfer constant (ESI, k_{heter}, $6.9x10^{-3}$ – $2.0x10^{-2}$ compared to $1.1x10^{-3}cms^{-1}$) reasonably attributable to the hindered phenanthrolines that limit the geometry modification around the Cu centre during the electron transfer and so lower the energy barrier. In the same conditions, apparent diffusion coefficients, D, are similar for all the investigated copper complexes (between $7\text{-}10\cdot10^{-6}$ cm^2 s^{-1}) but twice that for the Co^{2+} compound ($3.9\cdot10^{-6}$ cm^2 s^{-1}, Table S1), coherently with the lower coordination number of Cu and the absence of six bulky *t*-butyl substituents in the ligand sphere. In particular apparent diffusion coefficient of complex 5 ($1.04\cdot10^{-5}$ cm^2 s^{-1}) is in very good agreement with reported data [25, 30, 40], especially considering differences in both composition of working medium and electrochemical setup.

The **D2** dye is characterized by two subsequent reversible oxidation processes centred on the porphyrinic core, the first at $E_{1/2}$= 0.31 V *vs* $Fc^+|Fc$ in *N,N'*-dimethylformamide, similar to that reported for **D1** (0.29 V *vs* $Fc^+|Fc$) [34] (Supporting Information, Figure S8, Table S2).

Copper electrolytes (**1**/**2**-El, **3**/**4**-El and **5**/**6**-El; where El means electrolyte) were prepared dissolving the redox couple (0.17M Cu^{+}/0.017M Cu^{2+}) in CH_3CN with 0.1 M lithium trifluoromethanesulfonate as supporting salt and 0.25 M 4-*tert*-butylpyridine as additive to improve the V_{OC} of the devices. Control electrolytes I^-/I_3^--El and Cobalt-El were prepared with the same amount of electroactive species (see Experimental Section).

Results of the investigated thin film (ca. 6 μm) transparent DSSCs are presented in Table 2.

Table 2. Photoelectrochemical performances of DSSCs.[a]

Dye	Electrolyte	j_{SC} /mA cm^{-2}	V_{OC} /V	*FF*	PCE %
D1	1/2-El	5.9±0.1	0.81±0.01	0.77±0.01	3.7±0.1
D1	3/4-El	5.6±0.5	0.68±0.04	0.77±0.05	2.9±0.4
D1	5/6-El	3.5±0.2	0.86±0.05	0.70±0.03	2.1±0.2
D1	Cobalt–El	8.0±0.2	0.58±0.02	0.63±0.05	2.9±0.2
D1	I^-/I_3^--El	8.6±0.1	0.60±0.01	0.66±0.02	3.4±0.1
D2	1/2-El	4.8±0.3	0.75±0.03	0.74±0.04	2.7±0.3

[a]Under 100 mW cm^{-2} AM 1.5G irradiation; active area 0.20-0.25 cm^2; data are referred to at least two replicates.

Notwithstanding the lower V_{OC} **3**/**4**-El outperforms the Cu reference electrolyte **5**/**6**-El, confirming previous reports [28-28] and extending the potentiality of this copper redox couple towards a new class of dyes. Interestingly the new electrolyte **1**/**2**-El gives the best PCE (3.7%), with 28% and 75% increase of efficiency respect to **3**/**4**-El and **5**/**6**-El, respectively. A deeper characterization of the device performance and knowledge of the kinetics for the copper electron donation to the dye are mandatory to clarify the reasons for such a behaviour. In general all the monoelectronic couples based on coordination metal complexes exhibit, at comparable concentration, nearly unitary dye regeneration efficiencies (91-85%, Supporting Information, Table S3) and are superior to the equimolar iodide based electrolyte (71%). The best

regeneration, monitored at 650 nm, diagnostic for the formation of the oxidized dye, [33, 41] is found with **3/4-El** and **5/6-El**. The latter is characterized by a lower incident photon-to-current conversion with respect to the other redox mediators (Figure 1) but it has the strongest oxidative power of all the investigated electrolytes, with a related Fermi-level energy ($U_{F,redox}$) of –4.76 eV (Table 3 and Figure 2), and the longest lifetime (τ) for electrons in TiO_2 (Figure S9) resulting in the narrowest gap between the conduction band energy (U_{cb}) and the quasi-Fermi level of TiO_2 (U_{Fn}) within the explored series. This affords the highest percentage of photopotential conversion (Table 3). The highest total resistance of **5/6**-El (Figure S9), probably due to mass-transport limitations as previously reported [29], is a drawback that could explain the lowest photocurrent and the lower fill factor observed for the DSSC based on such electrolyte (Table 2).

The extremely high mass transport resistance seems to contrast with the comparable apparent diffusion coefficients of Cu(I) complexes (Table S1). However two important differences must be mentioned: i) in DSSC the diffusion-limiting species is actually the Cu(II) complex, being ten-fold less concentrated than Cu(I); ii) the presence of tbp seems to negatively affect the diffusion properties of copper complexes, both increasing the solution viscosity and directly interacting with Cu(II) species [25].

On the other hand, the 28% increase in PCE over **3**/**4**-El by **1**/**2**-El could be mainly attributed to its more positive redox potential (ΔE_{redox}= 0.10 V, Table 3) which leads to an increase of the V_{OC} from 0.68 to 0.81 V. In agreement with this thermodynamic explanation, comparable electron lifetime τ were obtained by EIS when reported as a function of U_{Fn} (Figure S9), along with a similar U_{cb}–U_{Fn} that suggests comparable charges in the two cells and hence comparable rate of recombination (Table 3). This last finding is in good agreement with the already mentioned comparable k_{heter} determined by EIS in a classical three-electrode cell (Table S1).

Figure 1. Top: polarization curves under 100 mW cm^{-2} AM 1.5G illumination (solid lines) and in dark (dashed lines) of **D1**-sensitized DSSCs. Bottom: photoaction spectra of the devices

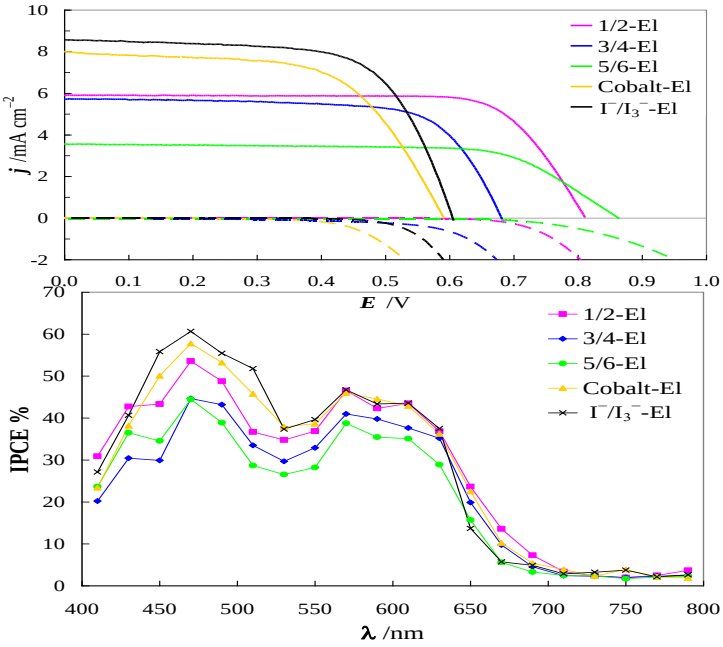

Table 3. E_{redox}, $U_{F,redox}$, U_{Fn}, and U_{cb}, at open circuit potential of **D1**-DSSCs.[a]

Electrolyte	E_{redox} *vs* Fc^+|Fc /V [b]	$U_{F,redox}$ /eV [c]	U_{Fn} /eV [d]	U_{cb} /eV [e]	U_{cb}–U_{Fn} /eV[f]	photopotential conversion %[f]
1/2-El	–0.10	–4.70	-3.89	–3.38	0.51	61
3/4-El	–0.20	–4.60	-3.92	–3.42	0.50	58
5/6-El	–0.04	–4.76	-3.90	–3.45	0.45	66
Cobalt–El	–0.28	–4.52	-3.94	–3.44	0.50	54
I^-/I_3^--El	–0.32	–4.48	-3.88	–3.40	0.48	55

[a] Under 100 mW cm^{-2} AM 1.5 G irradiation. [b] Determined through cyclic voltammetry as $E_{redox} = -E_{1/2,Fc+/Fc}$, measured as described in ESI. [c] Energy of the Fermi level of electrolyte, $U_{F,redox} = -e(E_{redox} + 4.8)$, with e the positive unit charge. [d] Quasi-Fermi level of TiO_2 at open circuit, evaluated as $U_{Fn} = U_{F,redox} + eV_{oc}$. [e] Conduction band edge energy at open circuit, calculated as reported in ESI. [f] Calculated comparing the generated photopotential V_{oc} respect to the theoretical maximum photopotential $(U_{cb}–U_{F,redox})/e$.

Figure 2. Energy diagram showing the energy levels useful to understand the cell operation.

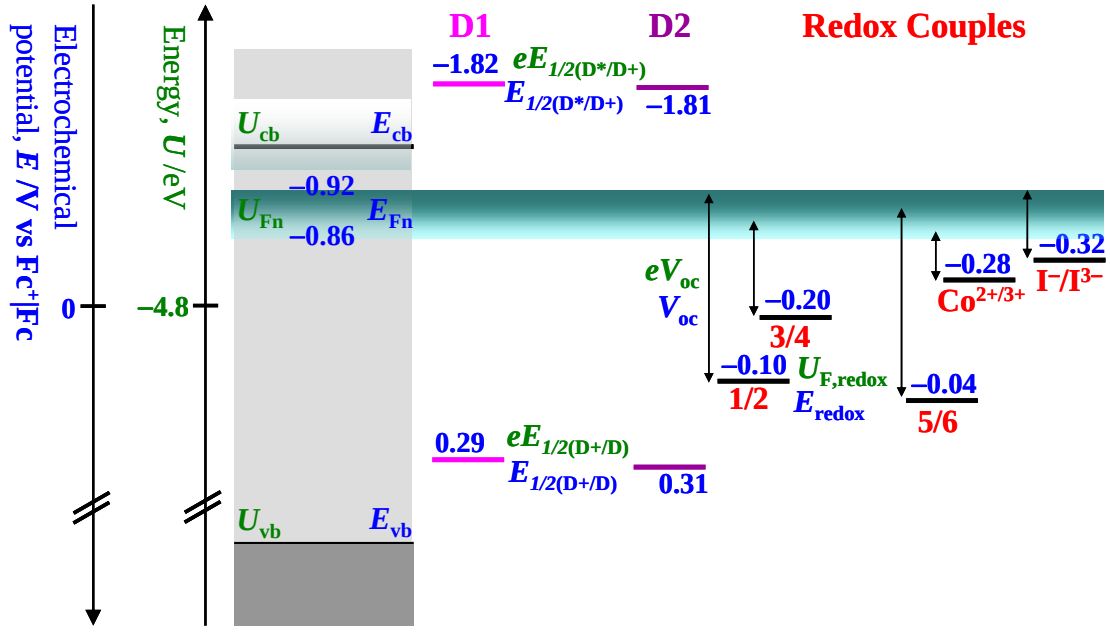

The great potential of the new **1**/**2** redox shuttle is confirmed by the PCE value (3.7%) of the related DSSC, much higher than that obtained with the reference electrolytes $[Co(dtb\text{-}bpy)_3]^{2+/3+}$ (2.9%) and comparable to I^-/I_3^- (3.4%), assuring a 200 mV increase of V_{oc}. The lower short circuit photocurrent, j_{sc}, of **1**/**2**-El cannot be attributed neither to a poorer dye regeneration (Figure S10) nor to any mass transport limitations as confirmed by dark-to-light chronoamperometric study (Figure S11) which records plateau current immediately after the light was switched off without occurring of any significant peak current attributable to diffusion-limited process. It could be attributed to competitive light harvesting of **1**/**2**-El with **D1**, as indicated by a relative 7-10% lower conversion efficiency at *ca* 460 nm, with respect to the reference electrolytes (Cobalt-El and I^-/I_3^-El) having a weaker absorption at this wavelength (Figure 1). On the other hand the Q band photoconversion, where Cu^+ MLCT absorption is

negligible, is nearly super-imposable in **1**/**2**-El and in the references. In any case, this lower light harvesting efficiency is more than counterbalanced by the Fermi energy of **1**/**2**-El ($U_{F,redox}$ = –4.70 eV, Table 3) with respect to both Cobalt-El and I^-/I_3^--El, resulting in a better V_{OC} which, together with the higher *FF*, leads to the best PCE value.

The best electrolyte **1**/**2**-El was finally tested with the **D2** Zn^{2+} porphyrin. Comparison with **D1** is reported in Figures 3 and S12. The constantly lower IPCE (Figure S12) together with the lower j_{sc} point towards a sluggish electron injection, notwithstanding the comparable energy of the $D^*|D^+$ excited state ($E_{1/2}(D^*|D^+$ = –1.82 and –1.81 V *vs* $Fc^+|Fc$ for **D1** and **D2**, respectively; Table S2). This behaviour can reasonably be explained by an energy increase of the conduction band edge with **D2**, leading to a lower driving force for the electron injection, attributable to the different nature of the anchoring group, being the electrolyte exactly the same.

Figure 3. Polarization curves under 100 mW cm^{-2} AM 1.5G illumination of **D2**-sensitized DSSCs, filled with **1**/**2**-El. For sake of comparison **D1**-sensitized cell is also reported.

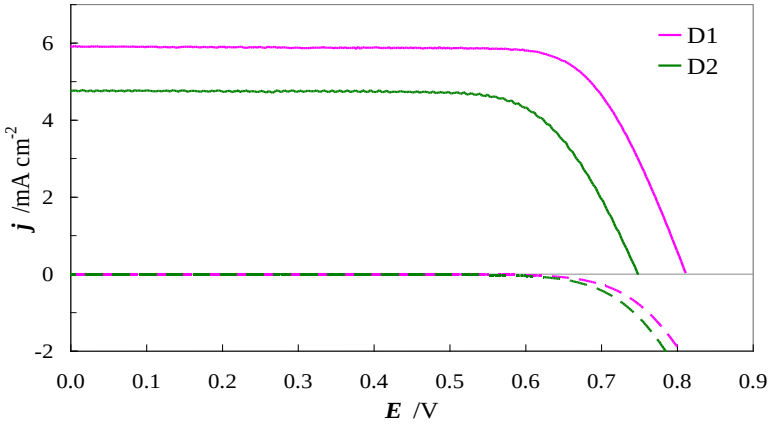

The 40 mV mismatch in V_{oc} (Figure S13) derived after simply shifting upward the *jE* curve of **D2** until j_{sc} matches that of **D1** (so virtually equalling charge injection fluxes) can roughly coincide with the conduction band shift [42], being dark currents quite superimposable. Moreover the lower V_{oc} for **D2**-photoanode is a direct consequence of the decreased injection which in turns downshifts the quasi-Fermi level, U_{Fn} (*i.e.* $eV_{oc}=U_{Fn}-U_{F,redox}$).

CONCLUSION

In conclusion this work has shown the great potential of Cu complexes that can be coupled with one of the most efficient classes of sensitizers, Zn^{2+} porphyrins in transparent solar cells. The new $[Cu(2\text{-mesityl-}1,10\text{-phenanthroline})_2]^{+/2+}$ **1**/**2** couple is particularly efficient when combined with **D1**, reaching a remarkable 75% increase of PCE with respect to the **5**/**6** Cu-reference thanks to a better diffusional behaviour. Removal of the electron releasing methyl groups from the positions 4,7 of the phenanthroline leads to an improvement of cell efficiency due to a quite high V_{oc}. Also, as a result of a more oxidizing $U_{F,redox}$, **1**/**2**-El neatly overcomes $[Co(dtb\text{-}bpy)_3]^{2+/3+}$ and I^-/I_3^- reference couples. Remarkably, Cu^+ complexes are efficient electron donors toward **D1**, reaching dye regeneration constants up to 2-fold and 4-fold faster than Co^{2+} and I^-, in equimolar conditions, respectively (Table S3). Thus, combination of β-substituted tetraaryl Zn^{2+} porphyrin dyes with copper-based redox mediators represents a novel route to low cost, environmental friendly DSSCs. This first report opens the way to new promising prospects through which optimization of electrolyte composition, copper complex

solubility, photoanode architecture and exploitation of other Zn^{2+}-porphyrins will surely result in a net improvement of DSSCs efficiencies.

ASSOCIATED CONTENT

Supporting Information.

Figures and tables related to the characterization of dyes and electrolytes; electrochemical, photoelectrochemical and transient absorption spectroscopy measurements.

AUTHOR INFORMATION

Corresponding Author

*E-mail: dominique.roberto@unimi.it

*E-mail: maddalena.pizzotti@unimi.it

*E-mail: stefano.caramori@unife.it

Author Contributions

The manuscript was written through contributions of all authors. All authors have given approval to the final version of the manuscript.

ACKNOWLEDGMENT

Regione Lombardia and Fondazione Cariplo are gratefully acknowledged for financial support and for the use of instrumentation purchased through the SmartMatLab Centre project (2014). AOB thanks Regione Lombardia (Accordo Quadro Regione Lombardia-CNR 2016, project: "I-ZEB Verso Edifici Intelligenti a Energia Zero per la crescita della città intelligente") for financial support.

DEDICATION

The strong belief of Professor Renato Ugo in the potential of coupling porphyrin dyes with copper electrolytes for DSSCs led to this paper that we dedicate to him on the occasion of his 79th birthday

REFERENCES

(1) O'Regan, B.; Grätzel, M. A low-cost, high-efficiency solar cell based on dye-sensitized colloidal TiO_2 films. *Nature* **1991**, *353*, 737-740.

(2) Grätzel, M. Recent Advances in Sensitized Mesoscopic Solar Cells. *Accounts Chem. Res.* **2009**, *42*, 1788-1798.

(3) Vougioukalakis, G. C.; Philippopoulos, A. I.; Stergiopoulos, T.; Falaras, P. Contributions to the development of ruthenium-based sensitizers for dye-sensitized solar cells. *Coord. Chem. Rev*. **2011**, *255*, 2602-2621.

(4) Li, L.-L.; Diau, E. W.-G. Porphyrin-sensitized solar cells. *Chem. Soc. Rev*. **2013**, *42*, 291-304.

(5) Colombo, A.; Dragonetti, C.; Valore, A.; Coluccini, C.; Manfredi,N.; Abbotto, A. Thiocyanate-free ruthenium(II) 2,2′-Bipyridyl complexes for dye-sensitized solar cells. *Polyhedron* **2014**, *82*, 50-56.

(6) Housecroft, C. E.; Constable, E. C. The emergence of copper(I)-based dye sensitized solar cells. *Chem. Soc. Rev*. **2015**, *44*, 8386-8398.

(7) Magni, M.; Biagini, P.; Colombo, A.; Dragonetti, C.; Roberto, D.; Valore, A. Versatile copper complexes as a convenient springboard for both dyes and redox mediators in dye sensitized solar cells. *Coord. Chem. Rev*. **2016**, *322*, 69-93 and references therein.

(8) Hamann, T. W.; Jensen, R. A.; Martinson, A. B. F.; Van Ryswykac H.; Hupp, J. T. Advancing beyond current generation dye-sensitized solar cells. *Energy Environ. Sci*. **2008**, *1*, 66-78.

(9) Wang, M.; Zakeeruddin S. M.; Grätzel, M. Recent developments in redox electrolytes for dye-sensitized solar cells. *Energy Environ. Sci*. **2012**, *5*, 9394-9405.

(10) Hamann, T. W. The end of iodide? Cobalt complex redox shuttles in DSSCs. *Dalton Trans*. **2012**, *41*, 3111-3115.

(11) Wu, J.; Lan, Z.; Lin, J.; Huang, M.; Huang, Y.; Fan, L.; Luo, G. Electrolytes in Dye-Sensitized Solar Cells. *Chem. Rev*. **2015**, *115*, 2136-2173.

(12) Pashaei, B.; Shahroosvand, H.; Abbasi, P. Transition metal complex redox shuttles for dye-sensitized solar cells. *RSC Adv.* **2015**, *5*, 94814-94848.

(13) Colombo, A.; Dragonetti, C.; Roberto, D.; Valore, A.; Biagini, P.; Melchiorre, F. A simple copper(I) complex and its application in efficient dye sensitized solar cells. *Inorg. Chim. Acta* **2013**, *407*, 204-209.

(14) Di Carlo, G.; Orbelli Biroli, A.; Pizzotti, M.; Tessore, F.; Trifiletti, V.; Ruffo, R.; Abbotto, A.; Amat, A.; De Angelis, F.; Mussini, P. R. Tetraaryl Zn^{II} Porphyrinates Substituted at β-Pyrrolic Positions as Sensitizers in Dye-Sensitized Solar Cells: A Comparison with meso-Disubstituted Push–Pull Zn^{II} Porphyrinates. *Chem. Eur. J.* **2013**, *19*, 10723-10740.

(15) Covezzi, A.; Orbelli Biroli, A.; Tessore, F.; Forni, A.; Marinotto, D.; Biagini, P.; Di Carlo, G.; Pizzotti, M. 4D–π–1A type β-substituted Zn^{II}-porphyrins: ideal green sensitizers for building-integrated photovoltaics. *Chem. Commun*. **2016**, *52*, 12642-12645.

(16) Urbani, M.; Grätzel, M.; Nazeeruddin, M.K.; Torres, T. Meso-substituted porphyrins for dye-sensitized solar cells. *Chem. Rev.* **2014**, *114*, 12330-12396.

(17) Mozer, A.J.; Wagner, P.; Officer, D.L.; Wallace, G.G.; Campbell, W.M.; Miyashita, M.; Sunahara, K.; Mori, S. The origin of open circuit voltage of porphyrin-sensitised TiO_2 solar cells. *Chem. Commun*. **2008**, 4741-4743.

(18) Griffith, M.J.; Sunahara, K.; Wagner, P.; Wagner, K.; Wallace, G.G.; Officer, D.L.; Furube, A.; Katoh, R., Mori,S.; Mozer, A.J. Porphyrins for dye-sensitised solar cells: new insights into efficiency-determining electron transfer steps. *Chem. Commun*., **2012**, *48*, 4145-4162.

(19) Chang, Y.-C.; Wang, C.-L.; Pan, T.-Y.; Hong, S.-H.; Lan, C.-M.; Kuo, H.-H.; Lo, C.-F.; Hsu, H.-Y.; Lin, C.-Y.; Diau, E.W.-G. A strategy to design highly efficient porphyrin sensitizers for dye-sensitized solar cells. *Chem. Commun*., **2011**, *47*, 8910-8912.

(20) Ripolles-Sanchis, T.; Guo, B.-C.; Wu, H.-P.; Pan, T.-Y.; Lee, H.-W.; Raga, S.R.; Fabregat-Santiago, F.; Bisquert, J.; Yeh, C.-Y.; Diau, E.W.-G. Design and characterization of alkoxy-wrapped push–pull porphyrins for dye-sensitized solar cells. *Chem Commun*. **2012**, *48*, 4368-4370.

(21) Wang, C.-L.; Lan, C.-M.; Hong, S.-H.; Wang, Y.-F.; Pan, T.-Y.; Chang, C.-W.; Kuo, H.-H.; Kuo, M.-Y.; Diau, E.W.-G.; Lin, C.-Y. Enveloping porphyrins for efficient dye-sensitized solar cells. *Energy Environ. Sci* **2012**, *5*, 6933-6940.

(22) Orbelli Biroli, A.; Tessore, F.; Vece, V.; Di Carlo, G., Mussini, P. R.; Trifiletti, V.; De Marco, L.; Giannuzzi, R.; Manca, M.; Pizzotti, M. Highly improved performance of Zn^{II} tetraarylporphyrinates in DSSCs by the presence of octyloxy chains in the aryl rings. *J. Mater. Chem. A* **2015**, *3*, 2954-2959 and references therein.

(23) Mathew, S.; Yella, A.; Gao, P.; Humphry-Baker, R.; Curchod, B. F.; Ashari-Astani, N.; Tavernelli, I.; Rothlisberger, U.; Nazeeruddin, M. K.; Grätzel, M. Dye-sensitized solar cells with

13% efficiency achieved through the molecular engineering of porphyrin sensitizers. *Nat. Chem*. **2014**, *6*, 242-247.

(24) Yella, A.; Mai, C. L.; Zakeeruddin, S. M.; Chang, S. N.; Hsieh, C. H.; Yeh C. Y.; Grätzel, M. Molecular engineering of push-pull porphyrin dyes for highly efficient dye-sensitized solar cells: the role of benzene spacers. *Angew. Chem., Int Ed*. **2014**, *53*, 2973-2977.

(25) Kavan, L.; Saygili, Y.; Freitag, M.; Zakeeruddin, S.M.; Hagfeldt, A.; Grätzel, M. Electrochemical properties of Cu(II/I)-based redox mediators for dye-sensitized solar cells. *Electrochim. Acta* **2017**, *227*, 194-202.

(26) Hattori, S., Wada, Y.; Yanagida, S.; Fukuzumi, S. Blue copper model complexes with distorted tetragonal geometry acting as effective electron-transfer mediators in dye-sensitized solar cells. *J. Am. Chem. Soc.* **2005***, 127*, 9648-9654.

(27) Bai, Y.; Yu, Q.; Cai, N.; Wang, Y.; Zhang, M.; Wang, P. High-efficiency organic dye-sensitized mesoscopic solar cells with a copper redox shuttle. *Chem. Commun*. **2011,** *47*, 4376-4378.

(28) Colombo, A.; Dragonetti, C.; Magni, M.; Roberto, D.; Demartin, F.; Caramori, S.; Bignozzi, C. A. Efficient Copper Mediators Based on Bulky Asymmetric Phenanthrolines for DSSCs. *ACS Appl. Mater. Interfaces* **2014**, *6*, 13945-13955.

(29) Magni, M.; Giannuzzi, R.; Colombo, A.; Cipolla, M. P.; Dragonetti, C.; Caramori, S.; Carli, S.; Grisorio, R.; Suranna, G. P.; Bignozzi, C. A.; Roberto, D.; Manca, M. Tetracoordinated Bis-phenanthroline Copper-Complex Couple as Efficient Redox Mediators for Dye Solar Cells. *Inorg Chem*. **2016**, *55*, 5245-5253.

(30) Freitag, M.; Giordano, F.; Yang, W.; Pazoki, M.; Hao, Y.; Zietz, B.; Grätzel, M.; Hagfeldt A.; Boschloo G. Copper Phenanthroline as a Fast and High-Performance Redox Mediator for Dye-Sensitized Solar Cells. *J. Phys. Chem. C* **2016**, *120*, 9595-9603.

(31) Magni, M.; Colombo, A.; Dragonetti, C.; Mussini, P Steric vs electronic effects and solvent coordination in the electrochemistry of phenanthroline-based copper complexes. *Electrochim. Acta* **2014**, *141,* 324 -330.

(32) Collini, E.; Mazzucato, S.; Zerbetto, M.; Ferrante, C.; Bozio, R.; Pizzotti, M.; Tessore F.; Ugo, R. Large two photon absorption cross section of asymmetric Zn(II) porphyrin complexes substituted in the meso or β pyrrolic position by –CC–C_6H_4X moieties (X = NMe_2, NO_2) *Chem. Phys. Letters* **2008**, *454*, 70-74.

(33) Di Carlo, G.; Caramori, S.; Trifiletti, V.; Giannuzzi, R.; De Marco, L.; Pizzotti, M.; Orbelli Biroli, A.; Tessore, F.; Argazzi, R.; Bignozzi, C. A. Influence of porphyrinic structure on electron transfer processes at the electrolyte/dye/TiO_2 interface in PSSCs: a comparison between meso push-pull and β-pyrrolic architectures. *ACS Appl. Mater. Interfaces* **2014**, *6*, 15841-15852.

(34) Magnano, G.; Marinotto, D.; Cipolla, M. P.; Trifiletti, V.; Listorti, A.; Mussini P. R.; Di Carlo, G.; Tessore, F.; Manca, M.; Orbelli Biroli, A.; Pizzotti, M. Influence of alkoxy chain envelopes on the interfacial photoinduced processes in tetraarylporphyrin-sensitized solar cells. *Phys. Chem. Chem. Phys*. **2016**, *18*, 9577-9585.

(35) Sapp., A. S.; Elliott, M. C.; Contado, C.; Caramori, S.; Bignozzi, C. A. Substituted polypyridine complexes of cobalt(II/III) as efficient electron-transfer mediators in dye-sensitized solar cells. *J. Am. Chem. Soc***. 2002** ,*124*, 11215-11222.

(36) Ronconi, F.; Santoni, M.P.; Nastasi, F.; Bruno, G.; Argazzi, R.; Berardi, S.; Caramori, S.; Bignozzi, C.A.; Campagna, S. Charge injection into nanostructured TiO_2 electrodes from the

photogenerated reduced form of a new Ru(II) polypyridine compound: the "anti-biomimetic" mechanism at work. *Dalton Trans*. **2016,** *45*, 14109-14123.

(37) Mba, M.; D'Acunzo, M.; Salice, P.; Carofiglio, T.; Maggini, M.; Caramori, S.; Campana, A.; Aliprandi, A.; Argazzi, R.; Carli, S.; Bignozzi, C. A. Sensitization of Nanocrystalline TiO2 with Multibranched Organic Dyes and Co(III)/(II) Mediators: Strategies to Improve Charge Collection Efficiency. *J. Phys. Chem. C* **2013**, *117,* 19885-19896.

(38) Trasatti, S. The absolute electrode potential: an explanatory note. *Pure & Appl. Chem.* **1986**, *58*, 955-966.

(39) Mandal D.; Hamann, T. W. Charge Distribution in Nanostructured TiO2 Photoanode Determined by Quantitative Analysis of the Band Edge Unpinning. *ACS Appl. Mater. Interfaces* **2016,** *8,* 419-424.

(40) Saygili, Y.; Söderberg, M.; Pellet, N.; Giordano, F.; Cao, Y.; Muñoz-García, A.B.; Zakeeruddin, S.M.; Vlachopoulos, N.; Pavone, M.; Boschloo, G.; Kavan, L.; Moser, J.E.; Grätzel, M.; Hagfeldt, A.; Freitag, M. Copper Bipyridyl Redox Mediators for Dye-Sensitized Solar Cells with High Photovoltage. *J. Am. Chem. Soc.* **2016** *138*, 15087−15096.

(41) Di Carlo, G.; Caramori, S.; Casarin, L.; Orbelli Biroli, A. Tessore, F.; Argazzi, R.; Oriana, A.; Cerullo, G.; Bignozzi, C.A.; Pizzotti, M. Charge Transfer Dynamics in β- and Meso-Substituted Dithienylethylene Porphyrins. *J. Phys. Chem. C.* **2017**, *121*, 18385–18400

(42) Barea, E. M.; Ortiz, J.; Paya, F. J.; Fernandez-Lazaro, F.; Fabregat-Santiago, F.; Sastre-Santos A.; Bisquert, J. Energetic factors governing injection, regeneration and recombination in dye solar cells with phthalocyanine sensitizers. *Energy Environ. Sci.* **2010**, *3*, 1985-1994.

Table of contents graphic and synopsis

TOC graphic

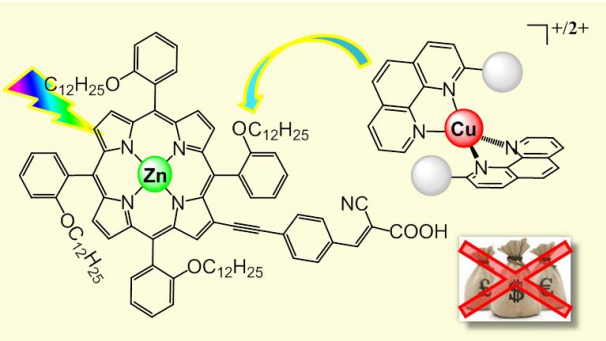

TOC SYNOPSIS

Combination of β-substituted Zn^{2+} porphyrin dyes and copper-based electrolytes represents a novel route for economic and environmentally friendly dye-sensitized solar cells. The new copper electrolyte, $[Cu(2\text{-mesityl-}1,10\text{-phenanthroline})_2]^{+/2+}$, exceeds the performance reached by $Co^{2+/3+}$ and I^-/I_3^- reference electrolytes.